

# A Mössbauer study of DyCrO<sub>4</sub> and ErCrO<sub>4</sub>

Cite as: AIP Advances 9, 035320 (2019); doi: 10.1063/1.5079989

Presented: 18 January 2019 • Submitted: 5 November 2018 •

Accepted: 8 January 2019 • Published Online: 14 March 2019



G. A. Stewart,<sup>1</sup> J. M. Cadogan,<sup>1</sup> W. D. Hutchison,<sup>1</sup> and D. H. Ryan<sup>2,a)</sup> 

## AFFILIATIONS

<sup>1</sup>School of Physical, Environmental and Mathematical Sciences, UNSW Canberra at the Australian Defence Force Academy, BC2610 ACT, Australia

<sup>2</sup>Physics Department and Centre for the Physics of Materials, McGill University, 3600 University Street, Montreal, Quebec H3A 2T8, Canada

**Note:** This paper was presented at the 2019 Joint MMM-Intermag Conference.

**a)**Corresponding author: D.H. Ryan [dhryan@physics.mcgill.ca](mailto:dhryan@physics.mcgill.ca)

## ABSTRACT

Earlier Mössbauer investigations of rare earth chromates RCrO<sub>4</sub> with R = Gd and Tm were interpreted in terms of a superposition of two sub-spectra (approx. 4:1 area ratio), despite there being only a single crystallographic R(4a) site. In addition, the magnetic transitions exhibited first-order character, which is contrary to bulk magnetic measurements. However, new <sup>161</sup>Dy and <sup>166</sup>Er Mössbauer data presented here for DyCrO<sub>4</sub> and ErCrO<sub>4</sub> show the expected single rare earth site in both cases and a conventional second order behaviour for ErCrO<sub>4</sub>.

© 2019 Author(s). All article content, except where otherwise noted, is licensed under a Creative Commons Attribution (CC BY) license (<http://creativecommons.org/licenses/by/4.0/>). <https://doi.org/10.1063/1.5079989>

## I. INTRODUCTION

The rare earth (R) chromates RCrO<sub>4</sub> have a tetragonal zircon-type structure (*I4<sub>1</sub>/amd*, #141). They are of interest because of competing ferromagnetic and antiferromagnetic super-exchange interactions between the 3d (Cr<sup>5+</sup>) and 4f (R<sup>3+</sup>) sites, believed to be responsible for the giant magnetocaloric effect observed recently for R = Gd, Dy and Ho.<sup>1,2</sup> Furthermore, the development of ferroelectric order associated with a transition to a non-centrosymmetric *I42d* structure has been observed around 100 K for R = Sm, Gd and Ho.<sup>3</sup>

In this tetragonal zircon-type structure the rare earth occupies a single, special (*i.e.* no free atomic position parameters) 4a crystallographic site but the rare-earth Mössbauer spectra for GdCrO<sub>4</sub><sup>4</sup> and TmCrO<sub>4</sub><sup>5</sup> all require two rare earth contributions with area ratios close to 4:1. These spectral contributions are well-resolved, exhibit quite different electric quadrupole interactions and, in the case of GdCrO<sub>4</sub>, even distinct ordering temperatures.<sup>4</sup> Prompted by these unexpected results, further rare-earth Mössbauer investigations are reported here for DyCrO<sub>4</sub> and ErCrO<sub>4</sub>. The key properties of these two chromates are summarized in Table I. They order ferromagnetically at  $T_c \sim 23$  K and 15 K, respectively, with the R and Cr moments directed in the basal plane. However, in the case of DyCrO<sub>4</sub>, this is preceded by a subtle orthorhombic structural transition with the moments confined to the b-axis. This is likely the case for ErCrO<sub>4</sub> as well. As pointed out by Steiner *et al.*<sup>6</sup> in an early neutron diffraction

study of DyCrO<sub>4</sub>, the only ferromagnetic group (*I4<sub>1</sub>/am'd'*) consistent with the zircon structure has the moments directed along the tetragonal c-axis (rather than in the basal plane).

## II. EXPERIMENTAL METHODS

The chromate samples were prepared using a nitrate precursor method<sup>7</sup> and Cu-K $\alpha$  x-ray powder diffraction confirmed them to be single-phase with lattice parameters of  $a = 7.1437(7)$  Å,  $c = 6.2741(7)$  Å for DyCrO<sub>4</sub> and  $a = 7.0862(8)$  Å,  $c = 6.232(1)$  Å for ErCrO<sub>4</sub>.

The <sup>161</sup>Dy 25.7 keV Mössbauer spectra were collected using an external, room temperature <sup>161</sup>Tb:<sup>161</sup>GdF<sub>3</sub> source ( $T_{1/2} = 6.9$  d) with the 80 mg/cm<sup>2</sup> DyCrO<sub>4</sub> absorber mounted in a conventional cold-tail cryostat. The sinusoidal drive velocity was calibrated against a reference Dy metal absorber. The <sup>166</sup>Er 80.56 keV spectra were recorded with both the <sup>166</sup>Ho:Ho<sub>0.4</sub>Y<sub>0.6</sub>H<sub>2</sub> source ( $T_{1/2} = 26.9$  h,  $T > 5$  K) and the 340 mg/cm<sup>2</sup> ErCrO<sub>4</sub> absorber mounted in a vertical configuration inside a Janis helium-flow cryostat. The drive velocity was calibrated using a He-Ne ( $\lambda = 632.8$  nm) laser interferometer.

## III. RESULTS AND DISCUSSION

### A. DyCrO<sub>4</sub>

The <sup>161</sup>Dy-Mössbauer spectra recorded for DyCrO<sub>4</sub> are shown in Figure 1. Above the ordering temperature of  $T_c = 23$  K, the spectra

**TABLE I.** Overview of structural and magnetic properties for DyCrO<sub>4</sub> and ErCrO<sub>4</sub>.

	DyCrO <sub>4</sub>	ErCrO <sub>4</sub>
T <sub>struct</sub> , T <sub>c</sub> , T <sub>SG</sub>	31.5 K, <sup>16</sup> 22–23 K, <sup>1,12,16</sup> 7–8 K <sup>1,12</sup>	15 K, <sup>17–19</sup> 6 K <sup>18</sup>
Crystal structure		
T > T <sub>struct</sub>	Tetragonal I <sub>4</sub> /amd, #141	Tetragonal I <sub>4</sub> /amd, #141
a, c (Å)	7.1375(3), 6.2656(3) (40 K) <sup>12</sup>	7.055(2), 6.193(8) (50 K) <sup>17</sup>
T < T <sub>struct</sub>	Orthorhombic Imma, #74	
a, b, c (Å)	7.1623(4), 7.1115(4), 6.2662(2) (3.6 K) <sup>12</sup>	
Magnetic structure	Orthorhombic Im'ma'	
μ(R), μ(Cr)	8.27(12), 0.79(7) μ <sub>B</sub> (b-axis) 3.6 K <sup>12</sup>	5.09, 0.91 μ <sub>B</sub> (ab-plane) 2 K <sup>17</sup>

show typical paramagnetic behaviour with the quadrupole splitting and Wegener relaxation broadening<sup>8</sup> diminishing as the temperature increases. Because of the broadening it is difficult to ascertain if there is more than one phase or Dy site at these temperatures. However, at T = 5 K, well below the ordering temperature, the magnetically-split absorption lines are well defined and described with a single spectrum. There is, therefore, no evidence of a second Dy site or phase for the DyCrO<sub>4</sub> specimen.

The 5 K spectrum was analyzed using a co-axial nuclear Hamiltonian of the form

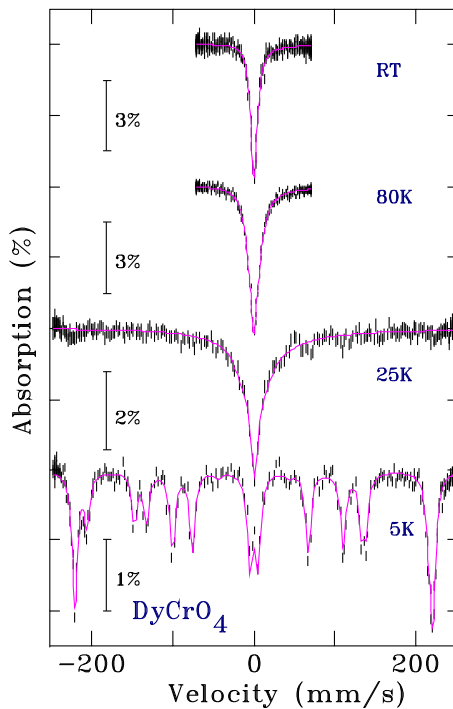


**FIG. 1.** <sup>161</sup>Dy-Mössbauer spectra recorded as a function of temperature for DyCrO<sub>4</sub>. The solid curve for T=5 K is a fit using the co-axial hyperfine interaction Hamiltonian described in the text. At higher temperatures, the spectra were fitted using an axial quadrupole interaction and the relaxation mechanism described by Wegener.<sup>8</sup> The dispersion term was fixed at the experimental value of  $\xi = -0.035$ .<sup>9</sup>

$$\mathcal{H} = \frac{\mu(I)B_{hf}}{I}I_z + \frac{eQV_{zz}(total)}{4I(2I-1)} \cdot [3I_z^2 - I(I+1)] \quad (1)$$

to describe the hyperfine splitting for each of the ground ( $I_g = \frac{5}{2}$ ) and excited ( $I_e = \frac{5}{2}$ ) nuclear levels of the E1, 25.7 keV, <sup>161</sup>Dy-Mössbauer transition. Adopting a ground state magnetic moment of  $\mu(I_g) = 0.4803(25) \mu_N$ ,<sup>10</sup> the fit to the DyCrO<sub>4</sub> spectrum at 5 K yields a magnetic hyperfine field of  $B_{hf} = 555(3)$  T. This is close to the free-ion value of  $B_{hf} = 559.8$  T<sup>11</sup> and corresponds to a local moment of  $\mu(Dy^{3+}) = 9.9(1) \mu_B$ , which lies within experimental error of the full, free-ion moment of  $\mu(FI) = gI = \frac{4}{3} \times \frac{15}{2} = 10\mu_B$ . However, the moment of  $\mu(Dy^{3+}) = 8.27(12)\mu_B$  determined using neutron diffraction by Long *et al.*<sup>12</sup> at 3.6 K is 17% smaller than the free ion moment. This suggests that the crystal field (CF) interaction dominates over a weaker exchange interaction to bring about a low-lying, exchange-split, Kramers doublet with thermally-fluctuating  $\pm 10\mu_B$  levels. <sup>161</sup>Dy-Mössbauer spectroscopy, with its time scale of the order of nanoseconds, samples the full, free-ion moment magnitude whereas neutron diffraction samples the thermally-averaged moment.

An estimate of the rank-2 CF parameter,  $B_2^0$ , can be obtained from the fitted electric-field gradient (efg). The fitted total efg value of  $V_{zz}(total) = 39.0(6) \times 10^{21} \text{ V/m}^2$  is considerably smaller than the expected free-ion value of  $V_{zz}(FI) = 55.3 \times 10^{21} \text{ V/m}^2$  (Ref. 11) due to a significant lattice contribution to the efg. In Eqn. 1 the quantization z-axis is defined as the direction of the total magnetic hyperfine field,  $B_{hf}$ , and the total “projected” efg is therefore given by

$$V_{zz}(total) = V_{zz}(4f) + \frac{1}{2}[3\cos^2\theta - 1]V_{zz'}(latt) \quad (2)$$

where  $\theta$  is the angle subtended by z and the principal axis,  $z'$ , of the lattice efg. The low temperature ( $T < 31.5$  K) orthorhombic (*Imma*, #74) structure determined by Long *et al.*<sup>12</sup> for DyCrO<sub>4</sub> deviates only slightly from its high temperature tetragonal (*I*<sub>4</sub>/amd) counterpart and it is reasonable to assume that the principal axis of the lattice efg remains closely associated with the (almost 4-fold symmetry) c-axis. Long *et al.*<sup>12</sup> also determined that the local Dy<sup>3+</sup> magnetic moment, and hence  $B_{hf}$ , is directed along the orthorhombic b-axis. Therefore, we can assume that  $\theta \sim 90^\circ$  and Eqn. 2 simplifies to

$$V_{zz}(total) = V_{zz}(4f) - \frac{1}{2}V_{cc}(latt) \quad (3)$$

which gives

$$V_{cc}(latt) = 2[V_{zz}(total) - V_{zz}(FI)] = +32.6 \times 10^{21} \text{ V/m}^2 \quad (4)$$

In the context of the point charge model approximation, and assuming no other contributions,  $V_{cc}(\text{latt})$  is given by<sup>13</sup>

$$V_{cc}(\text{latt}) = \frac{-4(1 - \gamma_\infty)}{|e|(1 - \sigma_2)\langle r^2 \rangle_{4f}} \times \frac{B_2^0}{\theta_2} \quad (5)$$

and this equation can be used to estimate the rank 2 CF parameter,  $B_2^0$ . Substituting values of  $(1 - \sigma_2) = 0.354$ ,  $\langle r^2 \rangle_{4f} = 0.67651 a_0^2$  and  $(1 - \gamma_\infty) = 60.97$  from Gupta and Sen<sup>14</sup> and  $\theta_2 = -0.006349$  from Stevens<sup>15</sup> gives  $B_2^0 = +6.6\text{K}$  with respect to the tetragonal c-axis. It is relatively straightforward to demonstrate that this rank 2 CF parameter would lead to the  $|\pm \frac{15}{2}\rangle$  level as the CF ground state with the z-axis aligned with the b-axis. However, for tetragonal site symmetry the magnetic exchange interaction and at least 4 higher rank CF terms (approximating as a local tetragonal symmetry) need to be taken into consideration.

## B. ErCrO<sub>4</sub>

The <sup>166</sup>Er-Mössbauer spectra recorded for ErCrO<sub>4</sub> as a function of temperature are shown in Figure 2. As for DyCrO<sub>4</sub>, the T = 5 K spectrum is well defined and, again, there is no indication of additional sites or phases. All spectra were analyzed using the co-axial nuclear Hamiltonian (Eqn. 1) to describe the hyperfine splitting of the excited ( $I_e = 2$ ) nuclear level of the E2, 80.6 keV, <sup>166</sup>Er-Mössbauer transition. Adopting an excited state magnetic moment of  $\mu(I_e) = 0.629(10) \mu_N$ ,<sup>20</sup> the magnetic hyperfine fields were determined and the results are presented in Figure 3 where the solid line is a fit to the temperature dependence using a  $J = \frac{15}{2}$  Brillouin function. The fitted

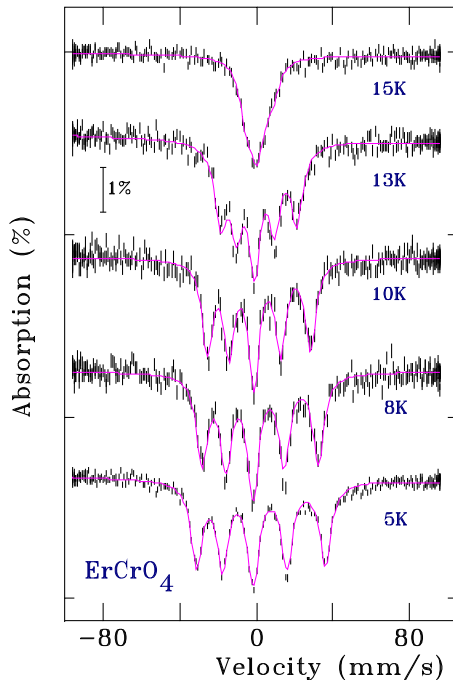


**FIG. 2.** <sup>166</sup>Er-Mössbauer spectra recorded as a function of temperature for ErCrO<sub>4</sub>. The solid lines are fits using the co-axial hyperfine interaction Hamiltonian described in the text.

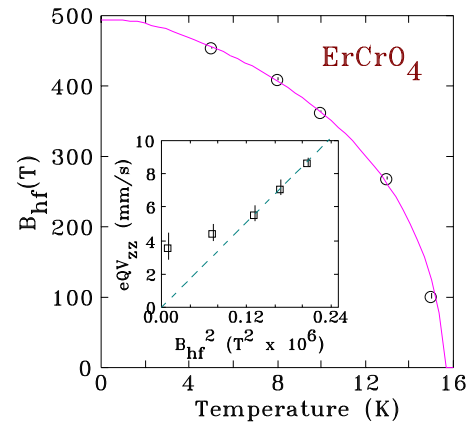


**FIG. 3.** Temperature dependence of the <sup>166</sup>Er hyperfine field in ErCrO<sub>4</sub>. The solid line is a fit to a  $J = \frac{15}{2}$  Brillouin function that yields an ordering temperature of 15.6(2) K. The low temperature linear relationship between  $eQV_{zz}$  and  $B_{hf}^2$  is highlighted in the inset.

ordering temperature of 15.6(2) K, is in excellent agreement with previously published values.<sup>17-19</sup>

At low temperatures (and hence large  $B_{hf}$  values)  $V_{zz}$  is dominated by the 4f contribution which is proportional to  $\langle J_z^2 \rangle$ , while  $B_{hf}$  is proportional to  $\langle J_z \rangle$ . Plotting the quadrupole interaction strength,  $eQV_{zz}$  vs.  $B_{hf}^2$  (inset to Figure 3) shows that this scaling does indeed apply for the three highest field points ( $T \leq 10$  K), and the fitted line passes through the origin.

Unlike the situation for DyCrO<sub>4</sub>, the extrapolated value of  $B_{hf}(T=0)$  is 495(10) T which is only 64% of the free-ion value of  $B_{hf} = 770.5$  T<sup>20</sup> and corresponds to a local moment of  $\mu(\text{Er}^{3+}) \sim 5.8(1) \mu_B$  (compared with the full, free-ion moment of  $\mu(\text{FI}) = gJ = \frac{6}{5} \times \frac{15}{2} = 9 \mu_B$ ). Unexpectedly, and contrary to the case for DyCrO<sub>4</sub>, this result is in reasonable agreement with the moment of  $\mu(\text{Er}^{3+}) = 5.09 \mu_B$  determined by Jiménez *et al.*<sup>19</sup> using neutron diffraction at 2 K.

Because the  $\text{Er}^{3+}$  ground state magnetic moment does not correspond to the full free-ion moment of  $9 \mu_B$ ,  $B_2^0$  cannot be calculated for ErCrO<sub>4</sub> with the approach used above for DyCrO<sub>4</sub>.

However, with the additional  $\text{Er}^{3+}$  values of  $(1 - \sigma_2) = 0.383$  and  $\langle r^2 \rangle_{4f} = 0.61886 a_0^2$  from Gupta and Sen,<sup>14</sup> and  $\theta_2 = +0.002540$  from Stevens,<sup>15</sup> it can be estimated via:

$$B_2^0(\text{Er}^{3+}) = \frac{[\theta_2(1 - \sigma_2)\langle r^2 \rangle_{4f}]_{\text{Er}^{3+}}}{[\theta_2(1 - \sigma_2)\langle r^2 \rangle_{4f}]_{\text{Dy}^{3+}}} \times B_2^0(\text{Dy}^{3+}) \approx -2.6 \text{ K}$$

to have the opposite sign and about 40% of the magnitude determined for DyCrO<sub>4</sub>.

## IV. CONCLUSIONS

Whereas the <sup>166</sup>Er-Mössbauer results for ErCrO<sub>4</sub> are in approximate agreement with the low temperature neutron diffraction determination of the  $\text{Er}^{3+}$  magnetic moment, the <sup>161</sup>Dy-Mössbauer results for DyCrO<sub>4</sub> are indicative of “slow” fluctuation of a fully-stretched CF ground doublet state. It remains unclear why, of the

five heavy rare earth systems with Mössbauer resonances, two (Gd and Tm) show two component spectra in approximately the same 4:1 area ratio, while the two investigated here (Dy and Er) are clearly single component. In view of this discrepancy we plan to revisit the Gd and Tm systems.

## ACKNOWLEDGMENTS

The thermal neutron activations of the Mössbauer sources were carried out at the Australian OPAL reactor, supported by AINSE grant #14547 ( $^{161}\text{Dy}$ ) and by M. Butler at the McMaster (Canada) Nuclear Reactor ( $^{166}\text{Er}$ ). Financial support for various stages of this work was provided by the Natural Sciences and Engineering Research Council of Canada and Fonds pour la formation de chercheurs et l'aide à la recherche, Québec.

## REFERENCES

- <sup>1</sup>A. Midya, N. Khan, D. Bhoi, and P. Mandal, *Appl. Phys. Lett.* **103**, 092402 (2013).
- <sup>2</sup>A. Midya, N. Khan, D. Bhoi, and P. Mandal, *J. Appl. Phys.* **115**, 17E114 (2014).
- <sup>3</sup>A. Indra, K. Dey, J. K. Dey, S. Majumdar, U. Rütt, O. Gutowski, M. v. Zimmermann, and S. Giri, *Phys. Rev. B* **98**, 014408 (2018).
- <sup>4</sup>E. Jiménez-Melero, P. C. M. Gubbens, M. P. Steenvoorden, S. Sakarya, A. Goosens, P. Dalmas de Réotier, A. Yaouanc, J. Rodríguez-Carvajal, B. Beuneeu, and J. Isasi, *J. Phys.: Condens. Matter* **18**, 7893 (2006).
- <sup>5</sup>E. Jiménez, P. C. M. Gubbens, S. Sakarya, G. A. Stewart, P. Dalmas de Réotier, A. Yaouanc, J. Isasi, R. Sáez-Puche, and U. Zimmermann, *J. Magn. Magn. Mater.* **272-276**, 568 (2004).
- <sup>6</sup>M. Steiner and H. Dachs, *Solid State Commun.* **29**, 231 (1979).
- <sup>7</sup>E. Jiménez, J. Isasi, and R. Sáez-Puche, *J. Alloys and Compounds* **312**, 53 (2000).
- <sup>8</sup>H. Wegener, *Z. für Physik* **186**, 498 (1965).
- <sup>9</sup>H. C. Goldwire and J. P. Hannon, *Phys. Rev. B* **16**, 1875 (1977).
- <sup>10</sup>P. Raghavan, *Atomic Data Nuclear Data Tables* **42**, 189 (1989).
- <sup>11</sup>G. A. Stewart, *Materials Forum* **18**, 177 (1994).
- <sup>12</sup>Y. W. Long, Q. Huang, L. X. Yang, Y. Yu, Y. X. Lv, J. W. Lynn, Y. Chen, and C. Q. Jin, *J. Magn. Magn. Mater.* **322**, 1912 (2010).
- <sup>13</sup>G. A. Stewart, *Hyperfine Interact.* **23**, 1 (1985).
- <sup>14</sup>R. P. Gupta and S. K. Sen, *Phys. Rev. A* **7**, 850 (1973).
- <sup>15</sup>K. W. H. Stevens, *Proc. Phys. Soc. A* **65**, 209 (1952).
- <sup>16</sup>K. Tezuka and Y. Hinatsu, *J. Solid State Chem.* **160**, 362 (2001).
- <sup>17</sup>R. Sáez-Puche, E. Jiménez, J. Isasi, J. Fernandez-Díaz, and J. L. García-Muñoz, *J. Solid State Chem.* **171**, 161 (2003).
- <sup>18</sup>Q. Y. Dong, Y. Ma, Y. J. Ke, X. Q. Zhang, L. C. Wang, B. G. Shen, J. R. Sun, and Z. H. Cheng, *Mater. Lett.* **161**, 669 (2015).
- <sup>19</sup>E. Jiménez, W. H. Kraan, N. H. van Dijk, P. C. M. Gubbens, J. Isasi, and R. Sáez-Puche, *Physica B* **350**, e293 (2004).
- <sup>20</sup>J. M. Cadogan and D. H. Ryan, *Hyperfine Interact.* **153**, 25 (2004).